SIMULATION OF FREE-ELECTRON LASER WITH HELICAL WIGGLER AND ION-CHANNEL GUIDING

F. Jafari Bahman, B. Maraghechi

Department of Physics, Amirkabir University of Technology, P. O. Box 15875-4413, Tehran, Iran

Abstract

Power and growth rate for free-electron laser amplifier with realizable helical wiggler and ion-channel guiding are calculated using a three-dimensional simulation with a steady-state amplifier model. The final form of dynamical field equations is obtained by substitution of the vector potential at Maxwell's equations. The electron orbit equations are derived by Lorentz force equation. The coupled nonlinear electron orbit equations and field equations have been solved numerically and finally, graph of power and growth rate are shown for TE_{11} mode

INTRODUCTION

Many studies on the free electron laser, in the long wavelength regime, have used axial static magnetic field to enhance the gain. Also, for low-energy and high current electron beam, axial magnetic field or ion channel guiding is used to focus the beam against the self-field. In ion-channel guiding, by passing the relativistic electron beam through the ionized plasma, the plasma electrons will be repelled by ions and the ion will remain stationary; this ion core will direct the beam. This technique was first proposed by Takayama and Hiramatsu [1] for use in free electron laser and was tested first by Ozaky et al [2], and was evaluated by the numerical simulation [3,4]. Theoretical studies for ion-channel guiding and helical wiggler under appropriate conditions have shown to produce significant power. Steady-state trajectories of electron for helical wiggler and ion-channel guiding have been studied in one and three dimensions [5-9]. In linear and nonlinear theory, many studies have been done on free electron laser with helical wiggler and ion-channel [10-12]. In nonlinear theory, free electron laser with helical wiggler and axial magnetic field has been studied by Ferund et al [13] but at the presence of realistic helical wiggler and ion-channel guiding in three dimensions, no calculation has been reported. This topic has been studied in this paper. Because of nonlinear calculations and three-dimensional form of the helical wiggler, the present analysis offers more accurate results compared to the one dimension at studies [10].

FIELD EQUATIONS

Helical wiggler magnetic field generated by a bifilar helix can be expressed in cylindrical coordinates as

$$\boldsymbol{B}_w(\boldsymbol{x}) = 2B_w(z)\left[\acute{I}_1(\lambda)\cos\chi\,\hat{\boldsymbol{e}}_{\boldsymbol{r}} - \frac{1}{\lambda}I_1(\lambda)\sin\chi\,\hat{\boldsymbol{e}}_{\boldsymbol{\theta}} + I_1(\lambda)\sin\chi\,\hat{\boldsymbol{e}}_{\boldsymbol{z}}\right] \quad (1)$$

where $B_w(z)$ denotes the wiggler amplitude, $k_w(=2\pi/\lambda_w)$ wiggler wave number, $\lambda \equiv k_w r$, $\chi = \theta - k_w z$, and I_n and $\acute{I}_n$denote the modified Bessel function of the first kind of order n and its derivative.

It is assumed that the wiggler amplitude varies adiabatically to model the injection of the beam by means of tapered wiggler amplitude,

$$B_w(z) = \begin{cases} B_w sin^2\left(\frac{k_w(z)}{4N_w}\right); & 0 \le z \le N_w\lambda_w \\ B_w; & N_w\lambda_w < z \le z_0 \end{cases} \quad (2)$$

Ion-channel electrostatic field is described as

$$\boldsymbol{E}_i(x,y) = 2\pi e n_i(x\hat{\boldsymbol{e}}_{\boldsymbol{x}} + y\hat{\boldsymbol{e}}_{\boldsymbol{y}}), \quad (3)$$

where n_i is the ion density.

In the absence of space-charge field, boundary conditions in waveguide are satisfied by vector potential expansion of orthogonal basis of cylindrical waveguide. Therefore, the vector potential radiation field is written as follows

$$\delta\boldsymbol{A}(\boldsymbol{x},t) = \sum_{l=0}^{\infty}\sum_{n=1}\delta A_{ln}(z)\left[\frac{1}{\kappa_{ln}r}J_l(\kappa_{ln}r)\sin\alpha_{ln}\hat{\boldsymbol{e}}_{\boldsymbol{r}} + \acute{J}_l(\kappa_{ln}r)\cos\alpha_{ln}\,\hat{\boldsymbol{e}}_{\boldsymbol{\theta}}\right], \quad (4)$$

for the TE modes, and

$$\delta\boldsymbol{A}(\boldsymbol{x},t) = \sum_{l=0}^{\infty}\sum_{n=1}\delta A_{ln}(z)\left[\acute{J}_l(\kappa_{ln}r)\cos\alpha_{ln}\,\hat{\boldsymbol{e}}_{\boldsymbol{r}} - \frac{1}{\kappa_{ln}r}J_l(\kappa_{ln}r)\sin\alpha_{ln}\hat{\boldsymbol{e}}_{\boldsymbol{\theta}} + \frac{\kappa_{ln}}{k_{ln}}J_l(\kappa_{ln}r)\sin\alpha_{ln}\hat{\boldsymbol{e}}_{\boldsymbol{z}}\right], \quad (5)$$

for TM modes, where for frequency ω and wave number $k_{ln}(z)$ we have

$$\alpha_{ln}(z) = \int_0^z d\acute{z}\ [k_{ln}(z) + l\theta - \omega t]. \quad (6)$$

in equations (5-6), J_l and $\acute{J}_l$ show the regular Bessel function of the first kind and its derivative, and κ_{ln} denote the cutoff wave number of each waveguide radius. For the

TE modes $\acute{J}_l(\acute{x}_{ln}) = 0$, $\kappa_{ln} \equiv \acute{x}_{ln}/R_g$ and for TM modes $J_l(x_{ln}) = 0$, $\kappa_{ln} \equiv x_{ln}/R_g$, and R_g is the waveguide radius.

DYNAMIC EQUATIONS OF EVOLUTION

The dynamic equations for the slowly varying amplitude and wave number of each mode are obtained by substitution of vector potential in Maxwell's equations

$$\left(\boldsymbol{\nabla}^2 - \frac{1}{c^2}\frac{d^2}{dt^2}\right)\delta\boldsymbol{A} - \boldsymbol{\nabla}(\boldsymbol{\nabla}.\delta\boldsymbol{A}) = -\frac{4\pi}{c}\delta\boldsymbol{J} \tag{7}$$

The microscopic source written as follows

$$\boldsymbol{J}(\boldsymbol{x},t) = -en_b v_{z_0}\iint_{A_g} dx_0 dy_0 \sigma_\perp(x_0,y_0) \times \int_{-T/2}^{T/2} dt_0\, \sigma(t_0)\boldsymbol{V}(z;x_0,y_0,t_0)\frac{\delta[t-\tau(z;x_0,y_0,t_0)]}{|v_z(z;x_0,y_0,t_0)|} \tag{8}$$

where v_{z_0} is the initial velocity of electron, $A_g\left(=\pi R_g^2\right)$ is the cross section of waveguide, $T = \mathrm{L}/v_{z0}$ is the period of electron beam pulse, $\sigma_\perp(x_0,y_0)$ and $\sigma(t_0)$ are distribution of initial conditions that may be obtained from normalization conditions

$$\iint_{A_g} dx_0 dy_0 \sigma_\perp(x_0,y_0) = A_g, \tag{9}$$

$$\int_{-\frac{T}{2}}^{\frac{T}{2}} dt_0\, \sigma(t_0) = T, \tag{10}$$

and the time of the electron at space z that enter interaction region at $z = 0$ and $(\mathrm{x_0}, \mathrm{y_0}, \mathrm{t_0})$ is

$$\tau(z;x_0,y_0,t_0) \equiv t_0 + \int_0^z \frac{d\acute{z}}{v_z(\acute{z};x_0,y_0,t_0)} \tag{11}$$

Substitution of microscopic fields and source current in Maxwell's equations and then averaging over wave period and orthogonalizing in r and θ, we obtain for TE modes

$$\frac{d\delta a_{ln}}{dz} \equiv \Gamma_{ln}\delta a_{ln}, \tag{12}$$

$$\frac{d\Gamma_{ln}}{dz} = -\left(\frac{\omega^2}{c^2} - k_{ln}^2 - \kappa_{ln}^2\right) + \frac{\omega_b^2 H_{ln}}{c^2\delta a_{ln}}\left\langle\frac{v_1 T_{ln}^{(+)} + v_2 w_{ln}^{(+)}}{|v_3|}\right\rangle, \tag{13}$$

$$\frac{dk_{ln}}{dz} = -2k_{ln}\Gamma_{ln} + \frac{\omega_b^2 H_{ln}}{c^2\delta a_{ln}}\left\langle\frac{v_1 w_{ln}^{(-)} - v_2 T_{ln}^{(-)}}{|v_3|}\right\rangle, \tag{14}$$

where $\delta a_{ln} = e\delta A_{ln}/mc^2$, $\omega_b^2 = 4\pi n_b e^2/m$, v_1 and v_2 are the transverse components of the electron velocity in rotating frame with wiggler.

$$\begin{cases}\hat{\boldsymbol{e}}_1 = \cos k_w z\,\hat{\boldsymbol{e}}_x + \sin k_w z\,\hat{\boldsymbol{e}}_y \\ \hat{\boldsymbol{e}}_2 = -\sin k_w z\,\hat{\boldsymbol{e}}_x + \cos k_w z\,\hat{\boldsymbol{e}}_y\end{cases} \tag{15}$$

H_{ln}, $T_{ln}^{(\pm)}$ and $W_{ln}^{(\pm)}$ are

$$H_{ln} = \frac{\acute{x}_{ln}^2}{(\acute{x}_{ln}^2 - l^2)J_l^2(\acute{x}_{ln})} \tag{16}$$

$$T_{ln}^{(\pm)} \equiv F_{ln}^{(\pm)}\sin\psi_{ln} + G_{ln}^{(\pm)}\cos\psi_{ln} \tag{17}$$

$$W_{ln}^{(\pm)} \equiv F_{ln}^{(\mp)}\cos\psi_{ln} - G_{ln}^{(\mp)}\sin\psi_{ln} \tag{18}$$

$$F_{ln}^{(\pm)} \equiv J_{l-1}(\kappa_{ln}r)\cos(l-1)\chi \pm J_{l+1}(\kappa_{ln}r)\cos(l+1)\chi \tag{19}$$

$$G_{ln}^{(\pm)} \equiv J_{l-1}(\kappa_{ln}r)\sin(l-1)\chi \pm J_{l+1}(\kappa_{ln}r)\sin(l+1)\chi \tag{20}$$

$$\psi_{ln} \equiv \psi_0 + \int_0^z d\acute{z}\left[k_{ln}(\acute{z}) + lk_w - \frac{\omega}{v_z}\right] \tag{21}$$

ψ_{ln} is the pondermotive phase and $\psi_0(=-\omega t_0)$ is the initial phase.

The average of beam electrons on axial phase and cross-section of waveguide is as fallow

$$\langle(\cdots)\rangle = \frac{1}{2\pi A_g}\int_{-\pi}^{\pi} d\psi_0\,\sigma(\psi_0)\iint_{A_g} dr_0 d\theta_0 r_0\sigma_\perp(r_0,\theta_0)(\cdots) \tag{22}$$

ELECTRON ORBIT EQUATIONS

The electron orbit equations can be obtained by substitution of the static fields in Lorentz force equation

$$v_z\frac{d\boldsymbol{P}}{dz} = -e\left[\boldsymbol{E}_i + \delta\boldsymbol{E} + \frac{\boldsymbol{V}}{c}\times(\boldsymbol{B}_w + \delta\boldsymbol{B})\right] \tag{23}$$

where $\delta\mathbf{E} = -\frac{1}{c}\frac{\partial}{\partial t}\delta\boldsymbol{A}$ and $\delta\boldsymbol{B} = \boldsymbol{\nabla}\times\delta\boldsymbol{A}$.

So the normalized components of velocities in wiggler frame are

$$\bar{v}_3\frac{d\bar{u}_1}{dz} = -\bar{\omega}_i^2(\bar{x}\cos\bar{z} + \bar{y}\sin\bar{z}) - \bar{u}_2\{2\bar{\Omega}_w I_1(\lambda)\sin\chi - \bar{v}_3\} + \bar{\Omega}_w\bar{u}_3 I_2(\lambda)\sin 2\chi - \sum_{l,n}\frac{\delta a_{ln}}{2}\left[(\bar{\omega} - \bar{k}_{ln}\bar{v}_3)w_{ln}^{(-)} - 2\bar{\kappa}_{ln}\bar{v}_2 J_l(k_{ln}r)\cos\alpha_{ln} + \bar{\Gamma}_{ln}\bar{v}_3 T_{ln}^{(+)}\right] \tag{24}$$

$$\bar{v}_3\frac{d\bar{u}_2}{dz} = -\bar{\omega}_i^2(\bar{y}\cos\bar{z} - \bar{x}\sin\bar{z}) + \{2\bar{\Omega}_w I_1(\lambda)\sin\chi - \bar{v}_3\}\bar{u}_1 - \bar{\Omega}_w\bar{u}_3[I_0(\lambda) + I_2(\lambda)\cos 2\chi] + \sum_{l,n}\frac{\delta a_{ln}}{2}\left[(\bar{\omega} - \bar{k}_{ln}\bar{v}_3)T_{ln}^{(-)} - 2\bar{\kappa}_{ln}\bar{v}_1 J_l(k_{ln}r)\cos\alpha_{ln} + \bar{\Gamma}_{ln}\bar{v}_3 w_{ln}^{(+)}\right] \tag{25}$$

$$\bar{v}_3\frac{d\bar{u}_3}{dz} = \bar{\Omega}_w\bar{u}_2[I_0(\lambda) + I_2(\lambda)\cos 2\chi] - \bar{\Omega}_w I_1(\lambda)\sin 2\chi\,\bar{u}_1 - \sum_{l,n}\frac{\delta a_{ln}}{2}\left[\bar{k}_{ln}\left(\bar{v}_1 w_{ln}^{(-)} - \bar{v}_2 T_{ln}^{(-)}\right) + \bar{\Gamma}_{ln}\left(\bar{v}_1 T_{ln}^{(+)} + \bar{v}_2 w_{ln}^{(+)}\right)\right] \tag{26}$$

$$\bar{\Gamma}_{ln} \equiv \frac{1}{\delta a_{ln}}\frac{d}{d\bar{z}}\delta a_{ln} \tag{27}$$

where $\bar{z} = k_w z$, $\bar{u} = \gamma\bar{v}$, $\bar{v} = v/c$, $\bar{\omega} = \omega/ck_w$, $\bar{k}_{ln} = k_{ln}/k_w$, $\bar{\kappa}_{ln} = \kappa_{ln}/k_w$, $\bar{\Omega}_w = eB_w/\gamma mc^2 k_w$, $\bar{\Gamma}_{ln} = \Gamma_{ln}/k_w$ and $\bar{\omega}_i^2 = 2\pi n_i e^2/mc^2 k_w^2$. We also have

$$\bar{v}_3 \frac{d\bar{x}}{dz} = \bar{v}_1 cos\,\bar{z} - \bar{v}_2 sin\,\bar{z} \quad (28)$$

$$\bar{v}_3 \frac{d\bar{y}}{dz} = \bar{v}_1 sin\,\bar{z} - \bar{v}_2 cos\,\bar{z} \quad (29)$$

$$\frac{d\psi_{ln}}{dz} = \bar{k}_{ln} + l - \frac{\bar{\omega}}{\bar{v}_3} \quad (30)$$

Here, there are three equations for velocity, (25-27), two equations for transverse space of electron, (28-29), and one equation for pondermotive phase, (30). These six nonlinear differential equations that are coupled together show the evolution of velocity and location of each electron. Equations (12-14, 27) show the evolution of amplitude and wave number of radiation. These equations must be solved numerically simultaneously.

RESULTS OF SIMULATION

The set of coupled nonlinear deferential equations for amplifier free-electron laser can be solved by forth order Runge-Kutta method.

The averages in the dynamical equations can be calculated by Nth order Gaussian quadrature technique for each (r_0, θ_0, ψ_0). We choose $N_r = N_\theta = N_\psi = 10$, so the simulation can be done for 1000 electrons.

It is clear that there is no energy spread in this calculation.

At first, it is assumed that a uniform and single energy electron beam with axial symmetry be injected into system. The electrons are picked within the ranges $-\pi \le \theta_0 \le \pi, 0 \le \psi_0 \le 2\pi, 0 \le R_0 \le R_{beam}$.

The initial growth rate for each mode is zero $[\Gamma_{ln}(z=0)=0]$ and we choose wiggler amplitude to increase from zero. The initial wave number is equivalent to vacuum $\left[k_{ln}(z=0) = (\omega^2/c^2 - \kappa_{ln}^2)^{\frac{1}{2}}\right]$.

For example, we select an amplifier with a 35GHz wide-band that works at TE_{11} mode. The parameters are: the amplitude of wiggler field $B_w = 2$kG, wavelength of wiggler $\lambda_w = 1.175$ cm; electron beam with energy 250kev, current 35A, initial radius $R_{beam} = 0.155$ cm; waveguide radius $R_g = 0.36626$ cm; input signal frequency $\bar{\omega} = 1.3$ and power P_{in}=10W [13]. Only TE_{11} mode is chosen in this simulation.

Table 1: FEL amplifier with a 35GHz wide-band works at $\boldsymbol{TE_{11}}$ mode.

wiggler	Amplitude	2 kG
	Wavelength	1.175 cm
Electron beam	Energy	250 kev
	Current	35 A
	Initial radius	0.155 cm
Waveguide	radius	0.36626cm
Input signal	frequency	1.3
	power	10W

In Figure 1, evolution of the radiation power as a function of axial position is presented for group I orbit parameters for ion-channel, $\bar{\omega}_i = 0.3$.

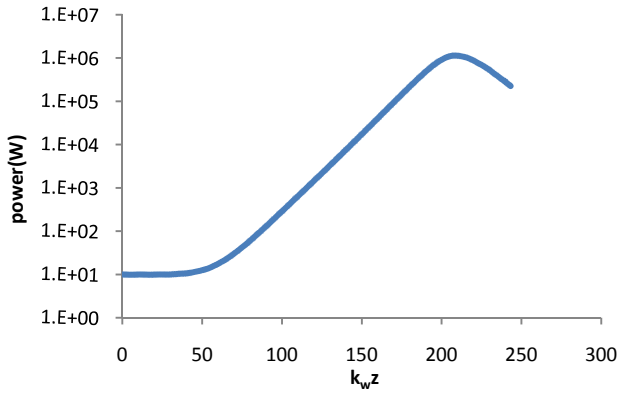

Figure 1: Evolution of the radiation power as a function of axial position.

Figure 2 shows the evolution of growth rate as a function of axial position for $\bar{\omega}_i = 0.3$.

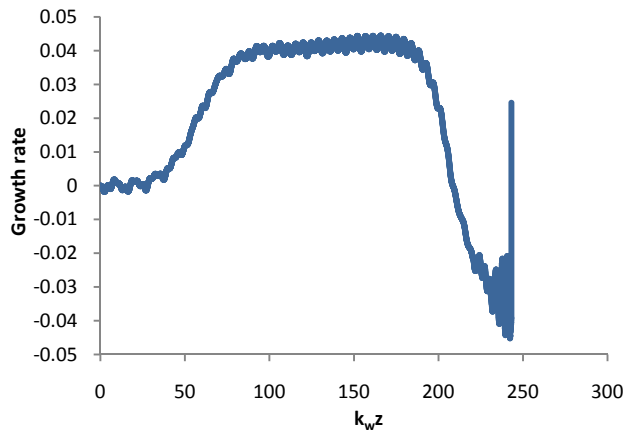

Figure 2: Evolution of the growth rate as a function of axial position.

As shown in Figure 1, power increases exponentially at $80.4 \le z \le 178$, and at this range the growth rate has a constant value, approximately equal to 0.04; This shows linear regime. Then power increases exponentially till z=207, which is the saturation point and radiation amplitude does not increase any more. This time, half of the electrons are confined in pondermotive potential wells, give energy to the wave and the other half receive energy from the wave. When both of them are equal, saturation is done. This then radiation amplitude does not increase and due to the reduced electrons energy, radiation amplitude decreases.

CONCLUSION

A three dimensional simulation of a free-electron laser in a steady-state amplifier model with negligible slippage

is performed. A general form for a helical wiggler is employed. An ion-channel is used for focusing of the beam against the self-fields as well as for the efficiency enhancement. Evolution of the radiation power and growth rate of TE_{11} mode is studied.

REFERENCES

[1] K. Takayama and S. Hiramatsu, Phys. Rev. A **37**, (1988) 173-177.

[2] T. Ozaki, K. Ebihara, S. Hiramatsu, J. Kishiro, T. Monaka, K. Takayama, and D. H. Whittum, Nucl. Instrum Methods Phys. Res. A **318**, (1992) 101-104.

[3] L. H. Yu, A. M. Sessler, and D. H. Whittum, Nucl. Instrum. Methods Phys. Res. A **318**, (1992) 721-725.

[4] P. Jha and J. S. Wurtele, Nucl. Instrum. Methods Phys. Res. A **331**, (1993) 477-481.

[5] P. Jha and P. Kumar, IEEE Trans. Plasma Sci **24**, (1996) 1359-1363.

[6] P. Jha and P. Kumar, Phys. Rev. E **57**, (1998) 2256-2261.

[7] M. Esmaeilzadeh, H. Mehdian, and J. E. Willett, Phys. Rev. E **65**, (2001) 016501-6.

[8] S. Mirzanejhad amd M. Asri, Phys. Plasmas **12**, (2005) 093108-8.

[9] S. Mirzanejhad, P. Maraghechi, and B. Maraghechi, Phys. Plasmas **11**, (2004) 3047-3052.

[10] A. Raghavi, G. D. Ninno, and H. Mehdian, Nucl. Instrum Methods Phys. Res. A **591**, (2008) 338-342.

[11] M. H. Rouhani and B. Maraghechi, Phys. Plasmas **16**, (2009) 093110-9.

[12] M. H. Rouhani and B. Maraghechi, Phys. Plasmas **17**, (2010) 023104-9.

[13] A. K. Ganguly and H. P. Freund, Phys. Rev. A **32**, (1985) 2275-2286.